

Porphyrin Effects on Zwitterionic HPS Micelles as Investigated by Small-Angle X-ray Scattering (SAXS) and Electron Paramagnetic Resonance (EPR)

Shirley C. M. Gandini,[†] Rosangela Itri,[‡] Diógenes de Sousa Neto,^{†,§} and Marcel Tabak^{*,†}

Instituto de Química de São Carlos, Universidade de São Paulo, Cx. Postal 780, CEP 13560-970, São Carlos, SP, Brazil, Instituto de Física da Universidade de São Paulo, Cx. Postal 66318, CEP 05315-970, São Paulo, SP, Brazil, and Instituto de Física de São Carlos, Universidade de São Paulo, São Carlos, SP, Brazil

Received: May 20, 2005; In Final Form: September 21, 2005

In this work, small-angle X-ray scattering (SAXS) and electron paramagnetic resonance (EPR) studies on the interaction of three anionic mesotetrakis (4-sulfonatophenyl) porphyrins, TPPS₄, FeTPPS₄, and ZnTPPS₄, at concentrations in the 2–10 mM range, with micelles of the zwitterionic surfactant 3-(*N*-hexadecyl-*N,N*-dimethylammonium) propane sulfonate (HPS, 30 mM) at pH 4.0 and 9.0 are reported. The SAXS results demonstrate that, upon addition of all species of porphyrins, the HPS micelle of prolate shape reduces its axial ratio from 1.8 ± 0.2 (in the absence of porphyrin) to 1.5 ± 0.1 . Such an effect is accompanied by a shrinking of the paraffinic shortest semiaxis from 22.5 ± 0.5 Å to 18.0 ± 0.2 Å. This shows that the micellar hydrophobic core is affected by porphyrin incorporation, independent of the type of porphyrin and pH. Concurrently, EPR results demonstrate an increase in the micellar packing as noticed from the increase in motional restriction for both nitroxides. Furthermore, increase of the porphyrin concentration induces the appearance of a repulsive interference function over the SAXS curve of zwitterionic micelles, which is typical of an interaction between surface-charged micelles. Such a finding gives strong evidence that the negatively charged porphyrin molecule must accommodate in the HPS micelle dipole layer close to the inner positive charges (near the hydrophobic core), inducing a surface charge (probably a negative one associated with the HPS sulfonate external groups) in the original zwitterionic (overall neutral) micelle. Such a porphyrin location is favored by both electrostatic and hydrophobic contributions, giving rise to binding constant values that are quite large compared to the binding of cationic drugs to HPS micelles (Caetano, W.; Barbosa, L. R. S.; Itri, R.; Tabak, M. *J. Coll. Int. Sci.* **2003**, 260, 414).

Introduction

Interaction of several solutes with the micellar phase and incorporation of biological-relevant molecules into micelles have been studied widely, implying that the micelles can, to some extent, be considered as a simple model for biomembranes.^{1–4}

Porphyrins are an important class of compounds that have been applied as therapeutic drugs and targeting agents in photodynamic therapy (PDT)^{5,6} and tumor localization.^{7,8} Metal derivatives (Me) of anionic mesotetra (4-sulfonatophenyl) porphyrin (MeTPPS₄) have been considered as prototypes for tumor-specific contrast agents in radiological and magnetic resonance imaging⁹ as well as catalysts in oxidation processes.¹⁰

The physicochemical and photophysical properties of porphyrins are associated with their structural characteristics that allow in many cases an effective interaction with the membrane matrix, involving localization of these molecules in different membrane environments.³ The physicochemical properties of porphyrins, such as spectroscopic features, protonation equilibrium constants, and ionization potentials, can be influenced deeply by the interaction with micellar and other model membrane systems.^{1–4,11}

In recent years, many efforts have been made to study porphyrin aggregation in both aqueous^{12–14} and micellar sur-

factant solutions.^{12,15–20} In particular, attempts have been made to use static, dynamic, and resonance light scattering to evaluate the size and shape of TPPS₄ aggregates at acidic conditions (usually at pH < 1) and micromolar porphyrin concentrations. A large number of porphyrin monomers ($N \approx 10^4$ – 10^5) in the aggregates assembling with a thin rod shape and very large dimensions has been determined.^{21,22} By using small-angle X-ray scattering (SAXS), TPPS₄ aggregates formed in aqueous solution at pH 4.0 and milimolar concentrations were modeled consistently by a hollow cylinder, where the monomer orientation and localization implies both the existence of J and H aggregates.¹³ The total number of porphyrin molecules in the whole aggregate was estimated as ~ 3000 . It is worthy of mention that this aggregate is very different from the one described by Collings et al.²¹ and Micali et al.,²² and this difference could be explained by the difference in pH value and porphyrin concentration; an increase of the porphyrin concentration has been associated with an increase in the complexity of the aggregated species in solution.¹⁴

Spectroscopic characterization of porphyrins interacting with different micelles has been also investigated by many researchers in the past few decades.^{4,12,15,23} Maiti et al.¹⁵ have reported that porphyrins interact with surfactants leading to stable structures of porphyrin-surfactant aggregates. The kinetics of the formation of the aggregates and its structure depend on attraction between the ionic surfactant and the opposite charge on the porphyrin. The structure of the porphyrin-surfactant aggregate depends

* Corresponding author. E-mail: marcel@sc.usp.br. Fax: 55-16-33739982.

[†] Instituto de Química de São Carlos.

[‡] Instituto de Física da Universidade de São Paulo.

[§] Instituto de Física de São Carlos.

on the concentration of the surfactant, and increasing this parameter leads to a sequential formation of J and H aggregates and, finally, solubilization of the porphyrin as monomers as shown in the following scheme: monomer \rightleftharpoons J \rightleftharpoons H \rightleftharpoons micellized monomer. In our previous work, we have studied the interaction of TPPS₄, FeTPPS₄, and ZnTPPS₄ with different surfactants.^{12,23} It has been shown that the mechanisms of porphyrin interaction imply both electrostatic and hydrophobic interactions with these systems. Our results have shown, in agreement with literature data,^{15,17} that these interactions depend on the surfactant headgroups and the pH of the medium.

The propensity of TPPS₄ to aggregate in acidic media, both in homogeneous solution,^{12,15,24} because of its transition to the diacid form: $\text{H}_2\text{TPPS}_4^{4-} + 2\text{H}^+ \rightleftharpoons \text{H}_4\text{TPPS}_4^{2-}$, and in the presence of cationic micelles^{12,15} is well known. For TPPS₄, the $\text{p}K_a = 4.52$ for micromolar concentrations in 20 mM acetate-phosphate buffer solution is changed in the presence of micelles. The value of $\text{p}K_a$ decreases to 2.56 for cationic cetyltrimethylammonium chloride (CTAC), whereas anionic sodium dodecyl sulfate (SDS) seems to cause a quite small, almost negligible, increase to $\text{p}K_a = 4.70$. Neutral polyoxyethylene lauryl ether (BRIJ-35) micelles induce a considerable decrease in $\text{p}K_a$, almost as great as CTAC ($\text{p}K_a = 2.80$). In the case of HPS, the absence of $\text{p}K_a$ has been associated with the partial protonation of the sulfonate groups of the surfactant, which are in large excess compared to porphyrin, in the used pH range.¹² In the case of FeTPPS₄, one of its most interesting characteristics is the formation of μ -oxygen bridged dimers, $\text{O}(\text{FeTPPS}_4)_2$. This metalloporphyrin usually exists as monomers in acid solutions and may form μ -oxo dimers upon alkalization.^{23,25,26} For FeTPPS₄ in 20 mM acetate-phosphate buffer solution, a $\text{p}K_d$ value of 7.2 was obtained, indicating a simple two-state equilibrium monomer–dimer. In the presence of micelles, values of $\text{p}K_d = 6.7$ for CTAC and 5.1 for neutral Triton X-100 micelles are observed.²³ However, zinc-sulfonated mesotetraphenylporphyrin ZnTPPS₄ is not supposed to form μ -oxygen bridged dimers, and no protonation equilibrium has been reported. These $\text{p}K_a$ and $\text{p}K_d$ changes of the porphyrins induced by the micelles are consistent with a strong porphyrin–micelle interaction. Association constants, K_b , on the order of 10^4 M^{-1} for all porphyrins with HPS were estimated and were very similar to those obtained for cationic CTAC.^{12,23}

Therefore, there is an interest concerning the protonation effects as well as porphyrin dimerization in the porphyrin–micelle interaction process. In this context, in the current work we make use of small-angle X-ray scattering (SAXS) to study isotropic micellar solutions composed of zwitterionic *N*-hexadecyl-*N,N*-dimethyl-3-ammonio-1-propanesulfonate (Figure 1, HPS 30 mM) at pH 4.0 and 9.0, in the absence and presence of increasing concentration of anionic mesotetrakis(4-sulfonatophenyl) porphyrins (TPPS₄) and its Fe(III) and Zn(II) complexes (Figure 1). According to the literature, zwitterionic HPS micelles have been described as small prolate ellipsoids.²⁷ The aim of this work is to investigate how the porphyrins impact the zwitterionic surfactant self-assembling in terms of micellar shape, size, and porphyrin/surfactant molar ratio. Furthermore, the effect that distinct porphyrin protonation and dimerization states have on the features of the micelles is also addressed. Finally, complementary electron paramagnetic resonance (EPR) spectroscopy experiments with stearic acid nitroxide derivatives 5-DSA and 16-DSA were performed to assess changes in the local dynamics of the scattering micelles under the influence of the porphyrins.

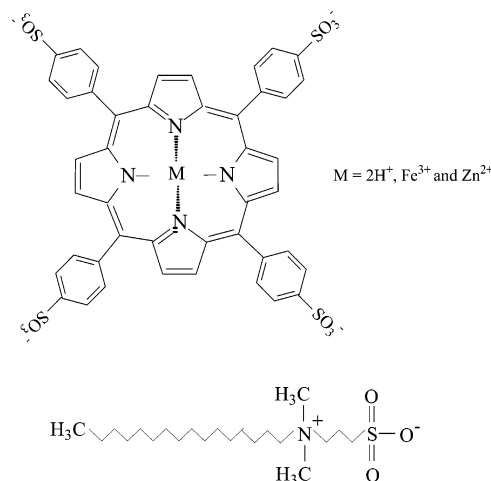


Figure 1. Chemical structures of mesotetrakis(4-sulfonatophenyl) porphyrin (TPPS₄) and its metallic derivatives of iron (III) (FeTPPS₄) and zinc(II) (ZnTPPS₄), and of zwitterionic HPS surfactant.

Experimental Section

Materials. The chloride salts of TPPS₄, ZnTPPS₄, and FeTPPS₄ (Mid-century), sodium acetate, sodium phosphate (Mallinckrodt), and zwitterionic HPS (Sigma) were used as received. The sample was prepared in 20 mM acetate/phosphate buffer using Milli-Q water. The pH values were adjusted with stock-concentrated calibrated solutions of HCl and NaOH and measured using a Digimed pH meter.

The samples for SAXS experiments were prepared in the following way: a weighted amount of porphyrins were dissolved in appropriate buffer to obtain a final porphyrin stock solution of 10 mM. The other concentrations were obtained by dilution of stock solution at 5 and 2 mM. Suspensions of detergent stock solutions of 0.2 M HPS, in buffer solution, were added to porphyrins solutions in Eppendorf tubes in order to obtain the desired porphyrin: HPS molar ratio at each chosen pH. Each sample had a final volume of 0.6 mL. The mixture was equilibrated for at least 48 h prior the experiments.

Samples for EPR experiments were prepared in the following way: small microliter aliquots of stock 10 mM ethanol solutions of nitroxide spin probes 5- and 16-doxyl stearic acids (Aldrich, used as received) were added to eppendorf test tubes. After drying the solvent, the mixtures of surfactant and porphyrins prepared in appropriate buffer as described above were added in such a way that the final nitroxide concentration was 10^{-4} M .

Methods. SAXS Data Analysis. SAXS measurements for solutions contained in a 1-mm-thick Mylar cell positioned perpendicular to the incident X-ray beam were performed at the National Laboratory of Synchrotron Light (LNLS, Campinas, Brazil). The samples were studied at room temperature ($22 \pm 1^\circ \text{C}$) with a radiation wavelength, λ , of 1.608 Å and a sample-to-detector distance of $\sim 600 \text{ mm}$. A one-dimension position-sensitive detector was used. SAXS curves were obtained with an acquisition time of 15 min. SAXS data were collected in the range $0.007 \text{ Å}^{-1} < q < 0.35 \text{ Å}^{-1}$ ($q = 4\pi \sin \theta / \lambda$ is the scattering vector; 2θ the scattering angle) and corrected for the parasitic scattering, which consisted of the buffer solution scattering taking into account the sample's attenuation factors, and detector inhomogeneity. No radiation damage was observed in these samples.

It is well known that the experimental small-angle X-ray scattering for particles of monodispersed size and shape distributed randomly in a colloidal solution can be modeled as²⁸

$$I(q) = k n_p P(q) S(q) \quad (1)$$

where $P(q)$ and $S(q)$ are the form factor and interparticle interference function, respectively; n_p is the scattering particle number density and k is a normalization factor related to the experimental setup. For $P(q)$, the micelle is modeled as a prolate ellipsoid made up of two shells of different electron densities:^{27,29,30} an inner core of paraffinic moiety with electron density $\rho_{\text{par}} = 0.275 \text{ e}/\text{\AA}^3$, and an external shell of thickness σ with electron density ρ_{pol} surrounding the core, containing the polar headgroups and the hydration water (free parameters), relative to the continuous medium (buffer solution with electron density assumed to be similar to the water $\rho_w = 0.327 \text{ e}/\text{\AA}^3$). The shortest semiaxis of the paraffinic core is R_{par} (free parameter) that is constrained to vary around the extended chain value ($\sim 21.0 \text{ \AA}$ for HPS^{27,31}), whereas the longest semiaxis is νR_{par} , with ν = axial ratio (another free parameter). Additional details can be found in ref 30.

$S(q)$ in eq 1 is equal to 1 for noninteracting systems and for porphyrin-free HPS micelles. However, for the mixed micelles at increasing porphyrin/HPS molar ratio, an interference function takes place over the SAXS curves. In these cases, the mixed aggregates can be associated with surface-charged micelles^{27,30} (ionization coefficient α , free parameter) interacting through a screened Coulomb potential in the mean spherical approximation (MSA).^{32,33} Accordingly, the micellar model used in $P(q)$ and the effective sphere for $S(q)$ have an equal inner-hydrocarbon-core volume and is surrounded by a polar shell of thickness σ . The structural parameters are then obtained by fitting eq 1 to the experimental data. The determination of k in eq 1 is performed by considering a scattering intensity for a sodium dodecyl sulfate micellar solution as a standard curve because the respective $P(q)$ and $S(q)$ parameters are well known.³⁴

Semiquantitative EPR Data Analysis. EPR spectra were run on a Varian E-9 spectrometer at room temperature using the following parameters: microwave frequency, 9.515 GHz; microwave power, 20 mW; center magnetic field, 340.5 mT; sweep width, 10 mT; sweep time, 2 min; modulation frequency, 100 kHz; modulation amplitude, 0.1 mT; detector time constant, 0.064 s. Samples were accommodated in microcapillary tubes sealed on both sides and adjusted inside a 3-mm EPR quartz tube. Quantitative estimates of molecular mobility by EPR were based on a previous approach described for small molecule–membrane interaction studies.^{35–37} The rotational correlation times of the nitroxide fragment for 16-DSA were calculated from the intensities of the three-component EPR spectra and line width of the central line as in ref 38. In the case of 5-DSA, the spectra are characteristic of a significant immobilization of radical motion precluding the use of this calculation. Qualitative assessment of probe mobility was made based on the intensity ratio of the low field line ($M_I = +1$) to the central line ($M_I = 0$) in the triplet spectra.³⁹

NLLS Simulation of EPR Spectra. EPR spectra simulations were performed by nonlinear least-squares (NLLS) fits, using the general slow-motional program.^{40,41} The magnetic g and a tensors are defined in a molecule-fixed frame, where the rotational diffusion rates around the x , y , and z axis are included.⁴¹ By convention, the x axis points along the N–O bond, the z axis is parallel to the $2p_z$ axis of the nitrogen atom, and the y axis is perpendicular to x and z .^{40,42} The fitting program NLLS permits one to estimate the rotational motion around axes x , y , and z (the diffusion tensor R) for a single or multicomponent EPR spectra. However, to reduce the number of free parameters and to simplify the simulation, we assume in some cases, as

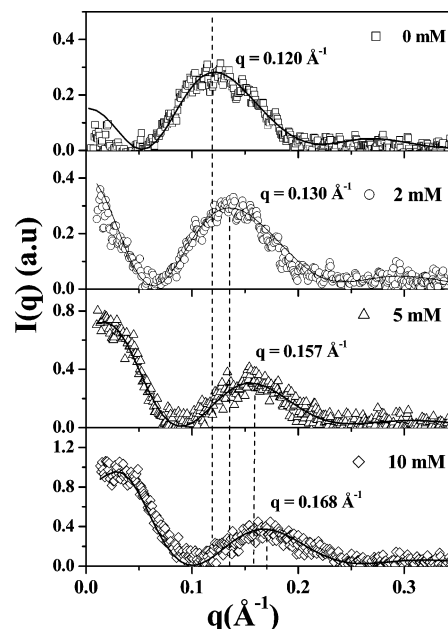


Figure 2. SAXS curves for 30 mM HPS at pH 9.0 as a function of TPPS₄ concentration indicated in the figure. The thick lines represent the best theoretical modeling (eq 1) in comparison to the experimental data (symbols). The adjustment parameters are described in Table 1.

described in ref 38, an axially symmetric rotational diffusion tensor with $R_{\text{bar}} = (R_{\perp}^2 R_{\parallel})^{1/3}$ and a rotational anisotropy with $R_{\parallel} = 10 R_{\perp}$.⁴¹ The magnetic parameters, g and a tensors, and additional line widths were optimized for all of the spectra simulated in this paper.

Results and Discussion

SAXS Data. Figure 2 shows the SAXS data obtained from 30 mM HPS, pH 9.0, in the absence and presence of increasing TPPS₄ concentration up to 10 mM. The thick lines represent the best modeling curves (eq 1). The scattering curves for pure surfactant micelles and for those containing 2 mM TPPS₄ are very similar at pHs 4.0 and 9.0. However, it was not possible to perform the studies for concentrations of 5 and 10 mM of TPPS₄ at pH 4.0 because of the intense sample precipitation in this particular experiment. It is noteworthy that previous results from 5 and 10 mM TPPS₄ demonstrated the presence of long tubular-like porphyrin aggregates in surfactant-free solutions at pH 4.0.¹³ Intermolecular electrostatic interaction is responsible for the assembling of large aggregates because of the stabilization between negatively charged sulfonate anions and positively charged porphyrin rings (Figure 1). At pH 9.0, the porphyrin rings are not positively charged and the aggregates are dissociated into smaller aggregates.¹³ The precipitation observed in this particular SAXS experiment at pH 4.0 seemed to suggest that the aggregation of the diprotonated porphyrins (H_4TPPS_4)²⁻ is enhanced by the complexation to HPS monomers leading to precipitation. However, further EPR studies described later on did not support this idea because the strong precipitation for the same samples was not observed.

Concerning the HPS micelles in the absence and presence of 2 mM TPPS₄, at pHs 4.0 and 9.0, the SAXS results show that the molecules assemble as small prolate ellipsoids with axial ratio $\nu = 1.8 \pm 0.2$ (Table 1), in good agreement with previous data obtained for HPS–phenothiazine compound aggregates.²⁷ The fittings to the experimental data were made without taking into account an intermicellar interference function ($S(q) = 1$ in eq 1) consistent with the null overall charge of zwitterionic micelles.

TABLE 1: Values of the Adjustment Parameters Obtained from the Scattering Curves of Samples Composed of 30 mM HPS, upon TPPS₄ Addition, through Prolate Ellipsoidal Form Factor $P(q)$ Modeling and Interference Function $S(q)$ (Eq 1)^a

| pH 4 | | | | | |
|---------------------------|----------------------|--------------|---|------------|----------|
| TPPS ₄ (mM) | R_{par} (Å) | σ (Å) | ρ_{pol} (e/Å ³) | ν | α |
| 0 | 22.5 (±0.5) | 7.4 (±0.1) | 0.400 (±0.002) | 1.8 (±0.1) | 0 |
| 2 | 21.0 (±0.5) | 6.9 (±0.2) | 0.400 (±0.003) | 1.7 (±0.1) | 0 |
| pH 9 | | | | | |
| TPPS ₄ (mM) | R_{par} (Å) | σ (Å) | ρ_{pol} (e/Å ³) | ν | α |
| 0 | 22.5 (±0.5) | 6.7 (±0.3) | 0.405 (±0.004) | 1.8 (±0.2) | 0 |
| 2 | 20.2 (±0.2) | 6.5 (±0.4) | 0.400 (±0.001) | 2.0 (±0.2) | 0 |
| 5 | 19.0 (±0.2) | 7.4 (±0.2) | 0.403 (±0.002) | 1.5 (±0.1) | 0.05 |
| 10 | 18.0 (±0.2) | 7.5 (±0.2) | 0.405 (±0.001) | 1.5 (±0.1) | 0.08 |

^a R_{par} = shortest paraffinic axis, σ = polar shell thickness, ρ_{pol} = polar shell electron density, ν = axial ratio between the largest and the shortest paraffinic axis, α = ionization coefficient.

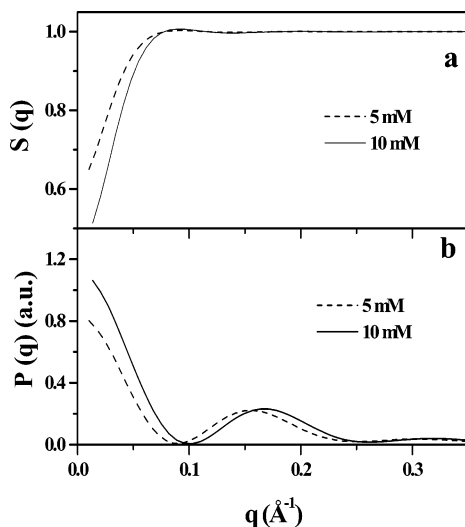


Figure 3. (a) Intermicellar interference function, $S(q)$, and (b) micellar form factor, $P(q)$, for SAXS curves of 30 mM HPS in the presence of TPPS₄ (5–10 mM) at pH 9.0.

However, as the TPPS₄ concentration increases at pH 9.0 (Figure 2), two important features can be noticed: first, the characteristic intramolecular peak with maximum intensity at $q_{\text{max}} = 0.120 \text{ Å}^{-1}$ ^{27,30} is shifted toward longer q values; second, a fairly interference peak takes place at shorter q values for porphyrin concentrations of 5 and 10 mM. The parameters obtained from the fittings to the SAXS data are displayed in Table 1. A perusal of the parameters indicates that the q_{max} displacement, evidenced in the $P(q)$ form factors in Figure 3b, is associated with a reduction of the shortest paraffinic axis, R_{par} , from $22.5 \pm 0.5 \text{ Å}$, which is consistent with the value reported previously for the drug-free micelle²⁷ and to the extended hexadecyl chain, to $R_{\text{par}} = 18.0 \pm 0.2 \text{ Å}$ upon incorporation of 10 mM TPPS₄, whereas the axial ratio bears a decrease to 1.5 ± 0.1 . Concurrently, a slight increase of polar shell thickness is also observed (σ changes from 6.7 ± 0.3 to $7.5 \pm 0.2 \text{ Å}$ (Table 1)), without any effect on polar head electron density ρ_{pol} . Therefore, our results show that the presence of the free-base charged porphyrin in HPS micelles, at pH 9.0, induces rearrangements in the system, favoring the formation of smaller HPS/TPPS₄ micelles with a slightly more packed hydrophobic core compared to the pure surfactant micelles.

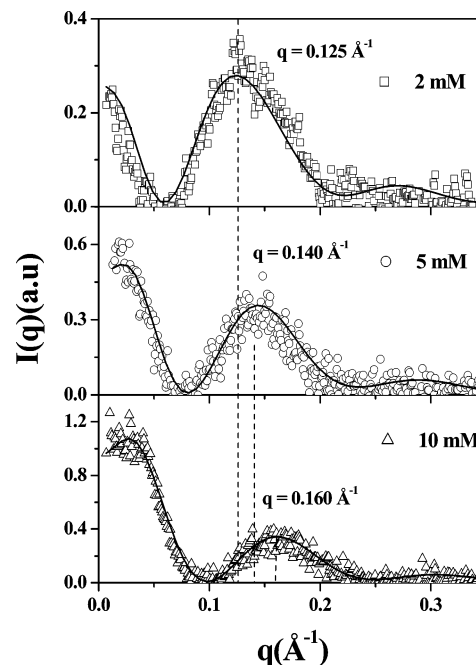


Figure 4. SAXS curves for 30 mM HPS at pH 4.0 as a function of ZnTPPS₄ concentration indicated in the figure. The thick lines represent the best theoretical modeling (eq 1) in comparison to the experimental data (symbols). The adjustment parameters are described in Table 2.

A striking result refers, however, to the appearance of an intermicellar interference factor as TPPS₄ concentration increases in the system at pH 9.0 (Figure 2). In Figure 3a, $S(q)$ values are shown separately for 30 mM HPS micelles in the presence of 5 and 10 mM of TPPS₄. As one can note, there is a small contribution of a repulsive interference function on the scattering curve because of the interaction between charged micellar surfaces. Furthermore, although the ionization coefficient, α , is small and must be considered as an effective parameter,²⁷ a slight increase in its value with drug addition in the system (α changes from 0.05 to 0.08 from 5 to 10 mM porphyrin, Table 1) indicates an increase in the surface charge of the mixed micelle. Then, the reduction of micelle size upon porphyrin association is consistent with an increase in micelle surface (mixed aggregate) charge and, as a consequence, to the repulsion of the components in the micelle. Furthermore, the highly charged porphyrin molecules (H_2TPPS_4)^{−4} must be placed mainly at the micellar polar shell, which barely affects its thickness, in such a way that they induce a non-null surface micelle charge distribution. Such drug location in the micelle must be driven by the surfactant electric dipole formed by positive and negative groups that must stabilize the formation of the negative charges of the porphyrin toward the positive charge of the zwitterions near the hydrophobic/hydrophilic interface (inner micellar interface).

In terms of metalloporphyrins, the effect that ZnTPPS₄ and FeTPPS₄ has on HPS micelles can be appreciated in Figures 4 and 5, respectively. The results are similar for both investigated pHs and, hence, just the results at pH 4.0 are presented. It is worthy of mention that for ZnTPPS₄ no changes are expected in the porphyrin properties as a function of pH in our studied range, whereas for FeTPPS₄ at pH 9.0 the formation of μ -oxo-dimer would imply that at this pH the interaction of the porphyrin dimer is being monitored as opposed to pH 4.0, where the porphyrin monomer is the single species in the solution.^{23,25} Tables 2 and 3 summarize the fitting parameters obtained from SAXS analysis for Zn- and Fe-based porphyrins, respectively.

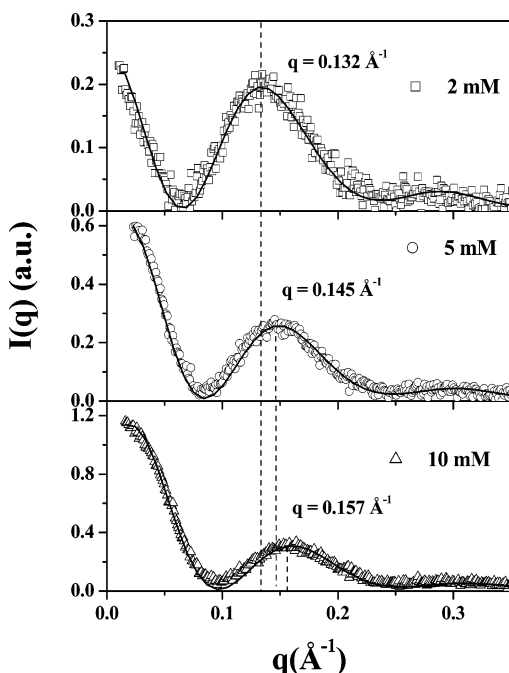


Figure 5. SAXS curves for 30 mM HPS at pH 4.0 as a function of FeTPPS₄ concentration indicated in the figure. The thick lines represent the best theoretical modeling (eq 1) in comparison to the experimental data (symbols). The adjustment parameters are described in Table 3.

TABLE 2: Values of the Adjustment Parameters Obtained from the Scattering Curves of Samples Composed of 30 mM HPS, upon ZnTPPS₄ Addition, through Prolate Ellipsoidal Form Factor $P(q)$ Modeling and Interference Function $S(q)$ (Eq 1)^a

| ZnTPPS ₄ (mM) | R_{par} (Å) | σ_{pol} (Å) | ρ_{pol} (e/Å ³) | ν | α |
|-----------------------------|----------------------|---------------------------|---|------------|----------|
| pH 4.0 | | | | | |
| 0 | 22.5 (±0.5) | 7.4 (±0.1) | 0.400 (±0.002) | 1.8 (±0.1) | 0 |
| 2 | 22.0 (±0.2) | 7.1 (±0.2) | 0.400 (±0.002) | 1.9 (±0.1) | 0 |
| 5 | 20.5 (±0.5) | 7.2 (±0.2) | 0.405 (±0.002) | 1.5 (±0.2) | 0.06 |
| 10 | 19.0 (±0.5) | 7.7 (±0.2) | 0.415 (±0.002) | 1.4 (±0.2) | 0.07 |
| pH 9.0 | | | | | |
| 0 | 22.5 (±0.5) | 6.7 (±0.3) | 0.405 (±0.004) | 1.8 (±0.2) | 0 |
| 2 | 21.5 (±0.4) | 7.0 (±0.2) | 0.400 (±0.003) | 1.7 (±0.1) | 0 |
| 5 | 19.5 (±0.5) | 7.7 (±0.3) | 0.401 (±0.004) | 1.4 (±0.1) | 0.06 |
| 10 | 18.0 (±0.2) | 7.7 (±0.3) | 0.410 (±0.004) | 1.4 (±0.1) | 0.06 |

^a R_{par} = shortest paraffinic axis, σ = polar shell thickness, ρ_{pol} = polar shell electron density, ν = axial ratio between the largest and the shortest paraffinic axis, α = ionization coefficient.

They are quite similar for all three porphyrins studied in this work. Then, the general trends observed for the free-base TPPS₄ also take place for these porphyrins: increase in metalloporphyrin concentration leads to a reduction of the HPS micellar size, reflected by a q_{max} shift of the micellar form factor to longer values, a decrease of the paraffinic radius and axial ratio, a small increase in polar shell thickness and, finally, an appearance of the interference function because of the presence of a high amount of porphyrin (5 and 10 mM). It should be remarked that, especially for 5 mM of Zn- and Fe-based porphyrin, some fitting trials were performed without taking into account the contribution of $S(q)$ (that was set equal to 1 in eq 1). Nevertheless, the fitting results were not satisfactory at a low q range, implying that a repulsive interaction between mixed micelles, although quite small, had to be included in the data analysis. It is worthy of mention that the polar shell electron density $\rho_{\text{pol}} = 0.400 \text{ e/Å}^3$ parameter remained practically unaltered with porphyrin concentration and pH, except for 10

TABLE 3: Values of the Adjustment Parameters Obtained from the Scattering Curves of Samples Composed of 30 mM HPS, upon FeTPPS₄ Addition, through Prolate Ellipsoidal Form Factor $P(q)$ Modeling and Interference Function $S(q)$ (Eq 1)^a

| FeTPPS ₄ (mM) | R_{par} (Å) | σ_{pol} (Å) | ρ_{pol} (e/Å ³) | ν | α |
|-----------------------------|----------------------|---------------------------|---|------------|----------|
| pH 4.0 | | | | | |
| 0 | 22.5 (±0.5) | 7.4 (±0.1) | 0.400 (±0.002) | 1.8 (±0.1) | 0 |
| 2 | 20.7 (±0.2) | 6.8 (±0.2) | 0.397 (±0.002) | 1.7 (±0.1) | 0 |
| 5 | 19.6 (±0.5) | 7.2 (±0.2) | 0.407 (±0.002) | 1.6 (±0.2) | 0.04 |
| 10 | 18.8 (±0.5) | 7.4 (±0.2) | 0.417 (±0.002) | 1.5 (±0.2) | 0.05 |
| pH 9.0 | | | | | |
| 0 | 22.5 (±0.5) | 6.7 (±0.3) | 0.405 (±0.004) | 1.8 (±0.2) | 0 |
| 2 | 21.0 (±0.3) | 6.9 (±0.2) | 0.398 (±0.003) | 1.7 (±0.2) | 0 |
| 5 | 19.6 (±0.5) | 7.3 (±0.3) | 0.407 (±0.004) | 1.6 (±0.1) | 0.05 |
| 10 | 18.5 (±0.2) | 7.9 (±0.3) | 0.418 (±0.004) | 1.4 (±0.1) | 0.06 |

^a R_{par} = shortest paraffinic axis, σ = polar shell thickness, ρ_{pol} = polar shell electron density, ν = axial ratio between the largest and the shortest paraffinic axis, α = ionization coefficient.

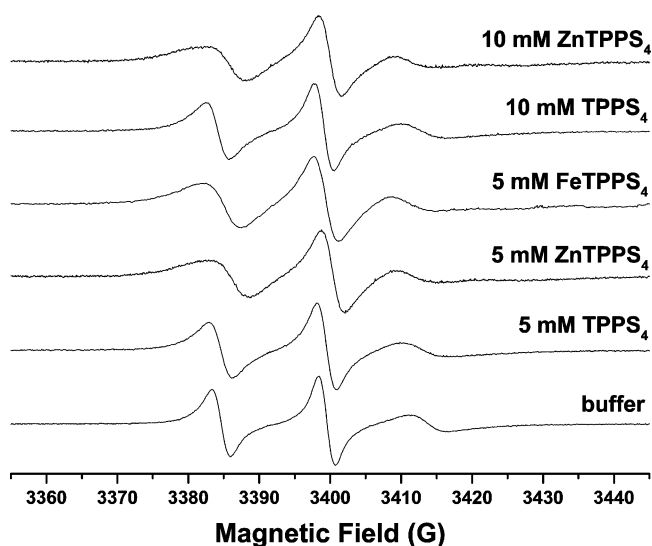


Figure 6. EPR spectra of 5-DSA in HPS 30 mM micelles at pH 4.0 in pure buffer and at the porphyrin concentrations indicated.

mM ZnTPPS₄ and FeTPPS₄, where the electron density increases to 0.415–0.418 e/Å³. Such finding reinforces the assumption that the charged porphyrins are located in the micellar surface, once the presence of the heavy metals in comparison to free-base molecule increases the polar shell electron density of the mixed micelle.

EPR Data. At this point it is worth commenting on the results obtained from EPR experiments with 5-DSA and 16-DSA for the effects of porphyrins in HPS micelle dynamics. In Figures 6 and 7, the EPR spectra of 5-DSA at pH 4.0 and 9.0, respectively, are shown for the indicated porphyrin concentrations. As can be noticed at pH 4.0, the spectra are typical for medium immobilization of the nitroxide in the micelle corresponding to a single component, whereas at pH 9.0 a spectral change is observed, consistent with either some further restriction of motion of 5-DSA in the micelles or the presence of a second component. As will be shown later on, simulation of the EPR spectra and analysis of the EPR parameters are more consistent with immobilization of the nitroxide at pH 9.0 and the presence of a single spectral component. In Figure 8, the EPR spectra of 16-DSA at pH 4.0 are presented. In this case, no significant difference was observed for the shape of EPR spectra at pH 9.0. In Table 4, data for 16-DSA are presented for the samples analyzed in this work. The EPR spectra (see

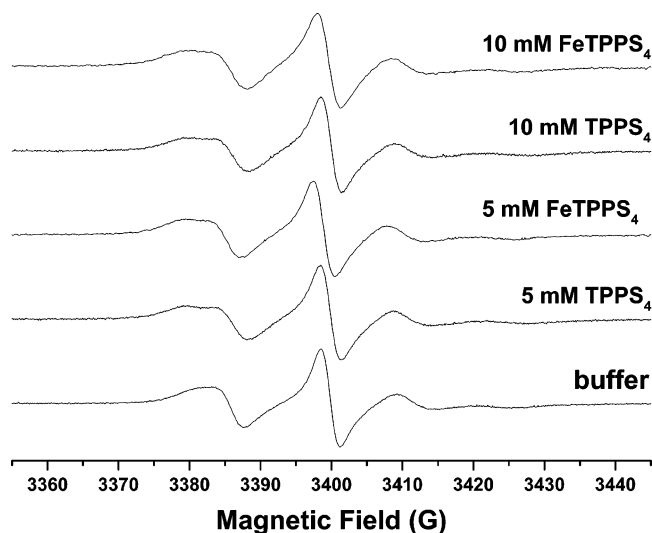


Figure 7. EPR spectra of 5-DSA in HPS 30 mM micelles at pH 9.0 in pure buffer and at the porphyrin concentrations indicated.

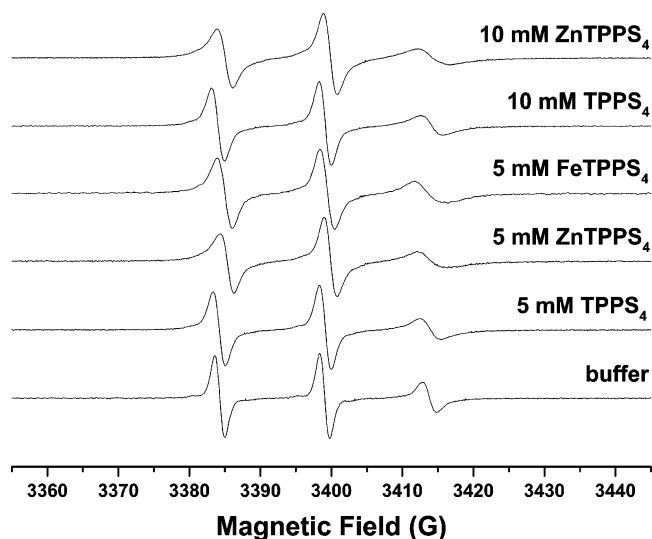


Figure 8. EPR spectra of 16-DSA in HPS 30 mM micelles at pH 4.0 in pure buffer and at the porphyrin concentrations indicated.

TABLE 4: Rotational Correlation Times τ_{2B} and τ_{2C} ($s, \times 10^9$) of the Nitroxyl Fragment of 16-DSA, Intensity Ratio h_{+1}/h_0 for 5-DSA in HPS 30 mM Micelles, and Values for Rotational Correlation Times Obtained from Diffusion Parameters R_{bar}^{-1} for 16-DSA and 5-DSA Based on Spectral Simulations with NLLS as Described in the Text

| solution composition | τ_{2B} | τ_{2C} | $R_{\text{bar}}^{-1}(16)/6$ | h_{+1}/h_0 | $R_{\text{bar}}^{-1}(5)/6$ |
|-----------------------------------|-------------|-------------|-----------------------------|--------------|----------------------------|
| pure HPS pH 4.0 | 1.03 | 1.12 | 0.22 | 0.50 | 0.91 |
| pure HPS pH 9.0 | 1.01 | 1.14 | 0.36 | 0.43 | 2.46 |
| +TPPS ₄ 5 mM pH 4.0 | 1.24 | 1.51 | 0.37 | 0.47 | 1.10 |
| +TPPS ₄ 10 mM pH 4.0 | 1.29 | 1.60 | 0.40 | 0.50 | 1.10 |
| +TPPS ₄ 5 mM pH 9.0 | 1.18 | 1.41 | 0.54 | 0.37 | 3.10 |
| +TPPS ₄ 10 mM pH 9.0 | 1.18 | 1.47 | 0.54 | 0.38 | 3.10 |
| +ZnTPPS ₄ 5 mM pH 4.0 | 1.38 | 1.65 | 0.63 | 0.48 | 2.52 |
| +ZnTPPS ₄ 10 mM pH 4.0 | 1.40 | 1.84 | 0.63 | 2.52 | |
| +FeTPPS ₄ 5 mM pH 4.0 | 1.12 | 1.29 | | 0.53 | 2.15 |
| +FeTPPS ₄ 5 mM pH 9.0 | 1.13 | 1.28 | 0.47 | 0.40 | 2.52 |
| +FeTPPS ₄ 10 mM pH 9.0 | 1.12 | 1.34 | 0.62 | 0.41 | 2.70 |

Figure 8) are in the limit of fast rotational motion and the estimated correlation times, τ_c , are all in the nanosecond range from 1.0–1.8 ns. It is seen that there is some motional anisotropy as deduced from the differences in τ_{2B} and τ_{2C} . Besides that, in the presence of all porphyrins the values of τ_c increase quite significantly, implying that the motion of 16-

DSA, which is located relatively deep in the hydrophobic micellar core, becomes more restricted compared to pure HPS micelles without porphyrin. This is consistent with an increase in packing of the micellar core. These results concerning the motion of 16-DSA are similar to previous data for 20 mM HPS micelles where the rotational diffusion parameter R_{bar}^{-1} was estimated as 3.5 ns.³⁸ Comparison of τ_c should be made with $(R_{\text{bar}}^{-1})/6$ as obtained from spectral simulation, so that the value of τ_c for 20 mM HPS is 0.6 ns, quite similar to the value for HPS 30 mM at pH 4.0/9.0 in Table 4 of 1.0 ns, estimated from intensities and line width. It is also apparent that for 10 mM porphyrin the increase of τ_c is the greatest, although in some cases the differences compared to 5 mM porphyrin are quite small. Interestingly, at 10 mM FeTPPS₄ (data not shown) at pH 4.0 the EPR spectrum is broadened considerably, almost completely losing its characteristic triplet structure. This effect is associated with the intense spin–spin interaction between the paramagnetic porphyrin in the monomeric form, where it is in a high spin state, and the nitroxide paramagnetic fragment, which is assumed to be in close enough contact with the porphyrin. In fact, for this sample (10 mM FeTPPS₄) both 16-DSA and 5-DSA nitroxides, at pH 4.0, present a similar severely broadened EPR spectrum, suggesting an effective spin–spin interaction independent of the position of the paramagnetic fragment, close to the interface or deeper in the micelle core. This is probably associated with the fact that micelles are very dynamic structures with a considerable degree of motion of the methylene chains of surfactants, making possible large fluctuations far from the classical picture of rigidly oriented chains with methyl terminals deep inside the hydrophobic core. The motion of the paramagnetic fragment of 16-DSA toward the interface is also possible and would contribute to its effective collision with the paramagnetic porphyrin.⁴³ In the case of 5-DSA, it was not possible to use the simplified procedure to estimate the rotational correlation times because the motion is not in the fast limit. The value for R_{bar}^{-1} was estimated previously for 5-DSA in pure 20 mM HPS micelles as nearly 40 ns using spectral simulation.³⁸ This would correspond to a τ_c value of 6.6 ns obtained from $\tau_c = (R_{\text{bar}}^{-1})/6$. In the present work, a qualitative procedure was performed using the ratio of intensities of low field to central lines in the triplet spectrum, h_{+1}/h_0 , and the data are also presented in Table 4. As can be seen, again motional restriction is observed for the nitroxide in the HPS micelles upon addition of porphyrins, as judged from the decrease of the intensity ratio. Just for comparison, h_{+1}/h_0 is equal to 0.91 and 0.76 for 16-DSA in pure HPS micelles at pH 4.0 and in the presence of 10 mM ZnTPPS₄, respectively. A significant increase in mobility is observed for the nitroxide located at the 16th carbon position in the methylene chain compared to 5-DSA, for which h_{+1}/h_0 varies from 0.53 to 0.38 (Table 4). However, the effect of porphyrins on the h_{+1}/h_0 parameter for 5-DSA is small, almost in the limit of error. The porphyrin effect becomes more evident only based on spectral simulations.

NLLS Spectral Simulation. In Table 4, the parameter $(R_{\text{bar}}^{-1})/6$ obtained from spectral simulations with the NLLS program is presented for both nitroxides. Simulation of EPR spectra was performed as described in the Methods section above. First, the magnetic parameters were optimized to obtain an initial rough simulation; then they were kept fixed and further optimization was performed by varying R_{bar} as a parameter and maintaining the ratio of $R_{\parallel}/R_{\perp} = 10$ also fixed. Finally, the magnetic parameters, and especially the nitrogen hyperfine tensor components, were allowed to change to reduce the overall

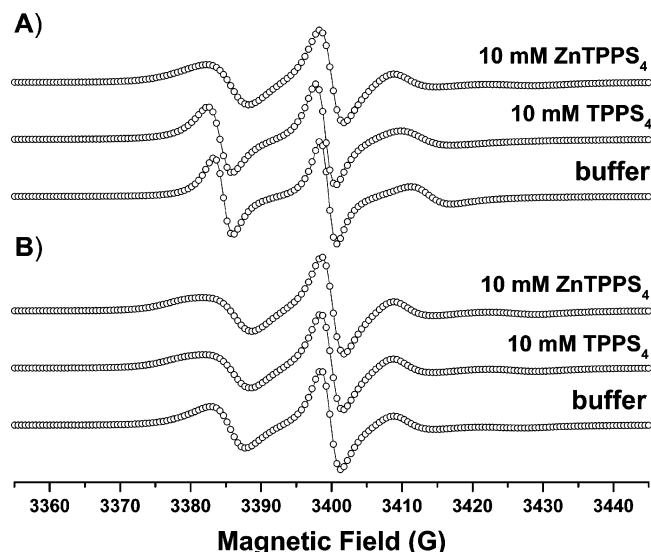


Figure 9. Experimental (circles) and simulated (lines) EPR spectra of 5-DSA in 30 mM HPS micelles in the absence and presence of the indicated porphyrin concentrations. EPR spectra in (A) correspond to pH 4.0 and in (B) to pH 9.0. The simulated spectra correspond to the best fit with NLLS program.

χ^2 , improve the final fitting, and get some idea of the polarity sensed by the nitroxide environment. A limitation of the NLLS program regarding the information on polarity sensed by the nitroxide is the fact that the only way to obtain it is through the hyperfine tensor components. In this way, very good fits were obtained, as shown for some EPR spectra in Figure 9, at pH 4.0 (Figure 9A) and pH 9.0 (Figure 9B). As mentioned above, the data at pH 4.0 are well simulated as a single component and the magnetic parameters are typical for nitroxides in micelles as described previously.³⁸ g -Tensor principal values were $g_{xx} = 2.0086$, $g_{yy} = 2.0060$, and $g_{zz} = 2.0029$ for both nitroxides in pure HPS micelles and did not change significantly in the presence of porphyrins. Simulation with the NLLS program allows one to obtain the diffusional tensor R_{bar}^{-1} from which rotational correlation times are estimated and compared, as well as the magnetic parameters, with special meaning for the value of the average nitrogen hyperfine tensor, a_0 , which is related to the polarity of the nitroxide environment. Principal components of the nitrogen hyperfine tensor were $a_{xx} = 6.30$, $a_{yy} = 5.86$, and $a_{zz} = 33.00$ G for pure HPS micelles, and a slight increase (about 0.2 G) was observed for increasing porphyrin concentrations. At pH 9.0, the g -tensor principal values were essentially the same as at pH 4.0. However, the nitrogen hyperfine tensor components were different, typically being equal to $a_{xx} = 7.36$, $a_{yy} = 7.50$, and $a_{zz} = 29.82$ G. This change suggests that the paramagnetic fragment of 5-DSA at alkaline pH is oriented in such a way that the contribution of electron density in the x and y directions is increased, whereas in the z direction it is reduced. From Table 4 it is clear that the motion of 16-DSA is significantly faster compared to 5-DSA, as expected. Besides that, the value of a_0 for both nitroxides is quite similar, being around 15.0 G for 5-DSA and 14.8 G for 16-DSA for pure surfactant. In the presence of porphyrins, a_0 tends to a slightly higher value around 15.1 ± 0.2 G and the differences are within the error limits. Two important features were observed from spectral simulations (see Table 4): first R_{bar}^{-1} and, as a consequence, τ_c increased upon addition of porphyrins; the second observation is that the polarity of the nitroxide was increased slightly upon addition of porphyrin. The data on polarity are consistent with the fact that 16-DSA senses a lower

polarity associated with its localization in a more hydrophobic environment compared to 5-DSA. Further, the increase of R_{bar}^{-1} as well as of polarity at pH 9.0 for 5-DSA compared to pH 4.0 could be associated with the fact that at pH 4.0 stearic acid nitroxide is protonated at the carboxyl group, being a neutral molecule, whereas at pH 9.0 it dissociates, becoming anionic. This would make it possible for 5-DSA to have some electrostatic interaction with the positive charge of HPS headgroup with consequent anchoring of the nitroxide at the polar shell and reduction of its overall mobility. Because at pH 9.0 both 5-DSA and 16-DSA will undergo deprotonation, for both of them R_{bar}^{-1} is increased compared to the value at pH 4.0. However, the reduction of mobility is more dramatic for 5-DSA because its paramagnetic fragment is located closer to the interface and the site of interaction. Attempts to model the EPR spectra at pH 9.0 with two components did not give meaningful results. Further, it is not clear how to interpret the existence of two components in a highly flexible system such as that of HPS micelles. So, this possibility has been left as a matter for future research.

Comparison of Porphyrin Effects with Phenothiazines.

The results described above for the anionic porphyrins are quite similar to our previous results monitoring the interaction of two phenothiazine compounds, trifluoperazine (TFP) and chlorpromazine (CPZ), with HPS.²⁷ In this case, both compounds, TFP and CPZ, are cationic and bear a positive charge under the pH studied in that work. A decrease of micellar size was also observed based on the reduction of both R_{par} and ν to values similar to those observed in the present work. The polar shell thickness did not change significantly for 30 mM HPS in the presence of up to 10 mM TFP or CPZ. Besides that, the interference function observed in the present work for high porphyrin concentrations of 5–10 mM was not present for the phenothiazines. This is certainly associated with the specific way that the drugs accommodate in the polar region of the micelle interacting with the charged micelle headgroups. Recent results of LPC micelles also reveal the appearance of an interference function because of the addition of a high concentration of cationic CPZ and TFP,⁴⁴ probably related to the inversion of the zwitterion dipole of this surfactant in respect to HPS.

It is noteworthy that for many ionisable compounds similar to porphyrins and phenothiazines we have found that their protonation behavior in the presence of HPS micelles is more similar to that either in the cationic CTAC or in neutral micelles, such as Triton X-100 or Brij-35, rather than in the anionic SDS one.^{12,23,27} The pK_a shifts induced by HPS are always in the same direction as those induced by either CTAC or neutral micelles and are contrary to the effect of SDS.^{27,45} This would suggest that in the zwitterionic HPS micelle the presence of the surfactant electric dipole formed by the positive and negative groups would stabilize the orientation of the negative charges of the porphyrin toward the positive charge of the surfactant headgroup; the accommodation of the neutral porphyrin ring relatively close to the surfactant sulfonate groups becomes possible because of the attenuation of the repulsion of the negative charges of the porphyrin by the presence of the positive (cationic tertiary amine groups) surfactant charges. This is not a pure electrostatic effect, as evidenced by the results for the phenothiazines, where CPZ, which has a different protonation behavior compared to TFP, presents similar effects on the micellar parameters of HPS. The binding constant of CPZ to HPS micelles is only slightly pH-dependent (varies from 457 M^{-1} at pH 2.0 to 668 M^{-1} at pH 7.0), whereas that for TFP is

strongly pH-dependent (increasing from 707 M^{-1} at pH 2.0 to 2247 M^{-1} at pH 7.0). So, for these compounds a factor of 3 or higher binding constant at pH 7.0 (equal charge states of $1+$) for TFP can be associated with a greater hydrophobicity, which is enough to preclude a significant binding reduction at pH 2.0, where TFP bears a $+2$ total charge compared to CPZ that has a charge of $+1$. Nevertheless, in the case of the porphyrins a substantial difference in comparison with the phenothiazines is observed as monitored by the appearance of the interference function at high porphyrin concentrations for all three species investigated in this work. Indeed, if for the phenothiazines there is a greater hydrophobic contribution for the binding of TFP compared to CPZ, then for all porphyrins used in this work the association constants to HPS are quite similar, implying that both electrostatic and hydrophobic contributions to the binding are also similar. In fact, the total charge of the porphyrins change as follows: for TPPS₄ it is -4 at pH 9.0 and -2 at pH 4.0, where the porphyrin ring is doubly protonated at the central ring nitrogens; for ZnTPPS₄ it is -2 , independent of pH, and finally for FeTPPS₄ it is -1 at pH 4.0 and probably -2 at pH 9.0 (the charge at pH 9.0 for the μ -oxo dimer would depend on the axial ligands that could be hydroxyl ions). The binding constants of TPPS₄ to HPS are $(2.6 \pm 0.5) \times 10^4 \text{ M}^{-1}$ at pH 3.0 and $(1.5 \pm 0.2) \times 10^4 \text{ M}^{-1}$ at pH 7.5;¹² for ZnTPPS₄ the binding constant at pH 4.0 is $(6 \pm 1) \times 10^4 \text{ M}^{-1}$;²³ and for FeTPPS₄ the binding constants are $(2.9 \pm 0.3) \times 10^4 \text{ M}^{-1}$ and $(1.2 \pm 0.2) \times 10^4 \text{ M}^{-1}$,²³ respectively, at pH 4.0 and pH 9.0. The higher binding constants of porphyrins compared to phenothiazines are probably due to the fact that both electrostatic and hydrophobic contributions are favored in this case. This occurs because, being anionic, the porphyrins tend to accommodate in the surfactant headgroup dipole layer close to the inner positive charges, that is, near the hydrophobic micellar core interface, being more tightly bound to HPS micelles; conversely, because the phenothiazines are cationic they are repelled from the inner positive charges and tend to accommodate more superficially in HPS micelles closer to the external negative sulfonate charges. The observation of a significant interference function is probably associated with the fact that a porphyrin molecule has four sulfonate groups and the accommodation of a single porphyrin in the micelle in close contact with the positive headgroup charges will contribute to induce a surface charge (probably a negative charge associated with the sulfonate external groups) in the original zwitterionic micelle. The greatest effect is indeed observed for TPPS₄ at pH 9.0 where the total porphyrin negative charge is the highest.

Conclusions

SAXS data for pure HPS and porphyrin/HPS mixtures have been modeled through the product $P(q)S(q)$, where $S(q)$ is the interparticle interference function and $P(q)$ is the orientational average of the particle form factor. The results are reproduced well by considering the micellar shape as represented by small prolate ellipsoid with parameters, quite similar to those described previously for pure HPS micelles.²⁷ The pH changes do not affect the hydrophobic core or the polar shell features of HPS micelles significantly. The addition of 2 mM TPPS₄, FeTPPS₄, and ZnTPPS₄ does not impact the characteristics of the micelles. However, at higher porphyrin concentrations (5 and 10 mM) the SAXS curves showed the presence of the intermicellar interference function, which increases as the porphyrin concentration increases, as well as a shift of the characteristic micellar peak at q around 0.125 \AA^{-1} to longer q values. The axial ratio reduces from 1.8 ± 0.2 to 1.4 ± 0.2 , and the

paraffinic shortest semiaxis ($22.5 \pm 0.5 \text{ \AA}$ for pure HPS micelles) also decreases by influence of all porphyrins ($18.0 \pm 0.2 \text{ \AA}$), showing that the micellar hydrophobic core is affected by drug incorporation, independent of the type of porphyrin and pH. The polar shell thickness, σ , increases as a function of porphyrin amount, especially at pH 9.0 (7.5 ± 0.2 , 7.7 ± 0.3 and $7.9 \pm 0.3 \text{ \AA}$ for TPPS₄, ZnTPPS₄ and FeTPPS₄, respectively). The analysis of SAXS data showed that the effects of all porphyrins on mixed micelles are quite similar, independent of the metal type compared to the free-base molecule. Porphyrin molecules are incorporated in the HPS micelles, slightly disrupting the paraffinic hydrophobic core, probably because of an additional hydrophobic contribution associated with the localization of the porphyrins in the polar shell, in close proximity to cationic groups of HPS, where electrostatic attraction and internal location would explain the observed high association constants. A decrease of the axial ratio in the porphyrin-HPS complex along with the appearance of an interference function suggests a more spherical shape environment for the mixed micelle, more packed than in the pure HPS micelles, as a result of both a stronger hydrophobic interaction because of the presence of porphyrins near the micelle inner interface and electrostatic interactions that lead to the reduction of the overall mixed micelle size. Simulation of EPR spectra for 5-DSA and 16-DSA allowed us to estimate the diffusion parameter, R_{bar}^{-1} , as well as the average polarity monitored by the nitroxides in the HPS micelles in the presence of porphyrins. All porphyrins induce an increase in motional restriction as well as a slight polarity increase, indicating more packed porphyrin-HPS micelles.

Acknowledgment. We are grateful to the staff of the SAXS beamline at the National Synchrotron Light Laboratory (LNLS, Campinas, Brazil) for support in the experiments. We thank FAPESP and CNPq for partial financial support. S.C.M.G. and D.S.N. are grateful to FAPESP for postdoctoral and M.Sc. fellowships, respectively. We are indebted to Dr. Antonio Alonso from Universidade Federal de Goiás, Goiânia, Brazil, and Dr. Carlos Ernesto Garrido Salmon from FFCLRP, USP, Ribeirão Preto, Brazil, for helpful discussions regarding the NLLS program.

References and Notes

- (1) Fendler, J. H. *Science* **1984**, 223, 888.
- (2) Zhang, Y. H.; Guo, L.; Ma, C.; Li, Q. L. *Phys. Chem. Chem. Phys.* **2001**, 3, 583.
- (3) Guo, L.; Liang, Y. Q. *Spectrochim. Acta, Part A* **2003**, 59, 219.
- (4) Scolaro, L. M.; Donato, C.; Castriciano, M.; Romeo, A.; Romeo, R. *Inorg. Chim. Acta* **2000**, 300–302, 978.
- (5) Dougherty, T. J.; Gomer, C. J.; Henderson, B. W.; Jori, G.; Kessel, D.; Korbely, M.; Moan, J.; Peng, Q. *J. Natl. Cancer Inst.* **1998**, 90, 889.
- (6) Bonnett, R. *Chem. Soc. Rev.* **1995**, 24, 19.
- (7) Berg, K.; Western, A.; Bommer, J.; Moan, J. *Photochem. Photobiol.* **1990**, 52, 775.
- (8) Kessel, D.; Thompson, P.; Saatio, K.; Nantwi, K. D. *Photochem. Photobiol.* **1987**, 45, 787.
- (9) Nelson, J. A.; Schmiedl, U. *Magn. Reson. Med.* **1991**, 22, 366.
- (10) Labat, G.; Séris, J. L.; Meunier, B. *Angew. Chem., Int. Ed. Engl.* **1990**, 29, 1471.
- (11) Fendler, J. H. *Membrane Mimetic Chemistry*; Wiley-Interscience: New York, 1982.
- (12) Gandini, S. C. M.; Yushmanov, V. E.; Borissevitch, I. E.; Tabak M. *Langmuir* **1999**, 15, 6233.
- (13) Gandini, S. C. M.; Gelamo, E. L.; Itri, R.; Tabak, M. *Biophys. J.* **2003**, 85, 1259.
- (14) Ribó, J. M.; Crusats, J.; Farrera, J. A.; Valero, M. L. *J. Chem. Soc., Chem. Commun.* **1994**, 681.
- (15) Maiti, N. C.; Mazumdar, S.; Periasamy, N. *J. Phys. Chem. B* **1998**, 102, 1528.

- (16) Maiti, N. C.; Mazumdar, S.; Periasamy, N. *Curr. Sci.* **1996**, 70, 997.
- (17) Kadish, K. M.; Maiya, G. B.; Araullo-McAdams, C.; Guillard, R. *Inorg. Chem.* **1989**, 28, 2725.
- (18) Kadish, K. M.; Maiya, G. B.; Araullo-McAdams, C. *J. Phys. Chem.* **1991**, 95, 427.
- (19) Tominaga, T.; Endoh, S.; Ishimaru, H. *Bull. Chem. Soc. Jpn.* **1991**, 64, 942.
- (20) Mazumdar, S.; Medhi, O. K.; Mitra, S. *Inorg. Chem.* **1988**, 27, 2541.
- (21) Collings, P. J.; Gibbs, E. J.; Starr, T. E.; Vafek, O.; Yee, C.; Pomerance, L. A.; Pasternack, R. F. *J. Phys. Chem. B* **1999**, 103, 8474.
- (22) Micali, N.; Mallamace, F.; Romeo, A.; Purrello, R.; Scolaro, L. *M. J. Phys. Chem. B* **2000**, 104, 5897.
- (23) Gandini, S. C. M.; Yushmanov, V. E.; Tabak, M. *J. Inorg. Biochem.* **2001**, 85, 263.
- (24) Pasternack, R. F.; Schafer, K. F.; Hambright, P. *Inorg. Chem.* **1994**, 33, 2062.
- (25) Fleischer, E. B.; Palmer, J. B.; Srivastava, T. S.; Chatterjee, A. *J. Am. Chem. Soc.* **1971**, 93, 3162.
- (26) Yushmanov, V. E.; Imasato, H.; Tominaga, T. T.; Tabak, M. *J. Inorg. Biochem.* **1996**, 61, 233.
- (27) Caetano, W.; Barbosa, L. R. S.; Itri, R.; Tabak, M. *J. Coll. Int. Sci.* **2003**, 260, 414.
- (28) (a) Bendedouch, D.; Chen, S. H. *J. Phys. Chem.* **1983**, 87, 1653. (b) Kotlarchyck, M.; Chen, S. H. *J. Chem. Phys.* **1983**, 79, 2461.
- (29) Marignan, J.; Basserau, P.; Delord, P. *J. Phys. Chem.* **1986**, 90, 645.
- (30) Caetano, W.; Gelamo, E. L.; Tabak, M.; Itri, R. *J. Coll. Int. Sci.* **2002**, 248, 149.
- (31) Teixeira, C. V.; Itri, R.; Casallanovo, F.; Schreier, S. *Biochim. Biophys. Acta* **2001**, 1510, 93.
- (32) Hayter, J. B.; Penfold, J. *Mol. Phys.* **1981**, 42, 109.
- (33) Hansen, J. P.; Hayter, J. B. *Mol. Phys.* **1982**, 46, 651.
- (34) (a) Itri, R.; Amaral, L. Q. *Phys. Rev. E* **1993**, 47, 2551–2557. (b) Itri, R.; Amaral, L. Q. *Phys. Rev. E* **1998**, 58, 1173. (c) Liu, Y. C.; Chen, S. H.; Itri, R. *J. Phys. A: Condens. Matter* **1996**, 8, 169.
- (35) Subczynski, W. K.; Markowska, E.; Gruszecki, W. I.; Sielewiesiuk, J. *Biochim. Biophys. Acta* **1992**, 1105, 97.
- (36) Yushmanov, V. E.; Imasato, H.; Perussi, J. R.; Tabak, M. *J. Magn. Reson. B* **1995**, 106, 236.
- (37) Alonso, A.; Meirelles, N. C.; Tabak, M. *Biochim. Biophys. Acta* **1995**, 1237, 6.
- (38) Gelamo, E. L.; Itri, R.; Alonso, A.; da Silva, J. V.; Tabak, M. *J. Colloid Interface Sci.* **2004**, 277, 471.
- (39) Schreier, S.; Frezzatti, W. A., Jr.; Araujo, P. S.; Chaimovich, H.; Cuccovia, I. M. *Biochim. Biophys. Acta* **1984**, 769, 231.
- (40) Schneider, D. J.; Freed, J. H. *Biological Magnetic Resonance*; Berliner, L. J., Reuben, J., Eds.; Plenum Press: New York, 1989; Vol. 8, pp 1–76.
- (41) Budil, D. E.; Lee, S.; Saxena, S.; Freed, J. H. *J. Magn. Reson.* **1996**, 120, 155–189.
- (42) *Spin Labeling: Theory and Applications*; Berliner, L. J., Ed.; Academic Press: New York, 1976.
- (43) Wasserman, A. M.; Kasaikin, V. A.; Timofeev, V. P. *Spectrochim. Acta, Part A* **1998**, 54, 2295.
- (44) Barbosa, L. R. S.; Caetano, W.; Itri, R.; Tabak, M., to be submitted for publication, 2005.
- (45) Caetano, W.; Tabak, M. *Spectrochim. Acta* **1999**, 55, 2513.